

General Disclaimer

One or more of the Following Statements may affect this Document

- This document has been reproduced from the best copy furnished by the organizational source. It is being released in the interest of making available as much information as possible.
- This document may contain data, which exceeds the sheet parameters. It was furnished in this condition by the organizational source and is the best copy available.
- This document may contain tone-on-tone or color graphs, charts and/or pictures, which have been reproduced in black and white.
- This document is paginated as submitted by the original source.
- Portions of this document are not fully legible due to the historical nature of some of the material. However, it is the best reproduction available from the original submission.



Technical Memorandum 79674

Intense Magnetic Fields At 1AU: Solar Cycle 20

(NASA-TM-79674) INTENSE MAGNETIC FIELDS AT
1 AU: SOLAR CYCLE 20 (NASA) 33 p HC A03/MF
A01 CSCL 03B

N79-13969

Unclas
40942

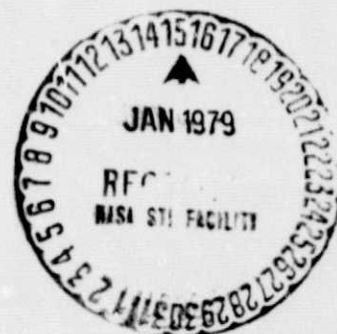
G3/90

L. F. Burlaga and J. H. King

November 1978

National Aeronautics and
Space Administration

Goddard Space Flight Center
Greenbelt, Maryland 20771



Intense Magnetic Fields at 1 AU:
Solar Cycle 20

L. F. Burlaga
J. H. King
NASA/GSFC
Laboratory for Exterrestrial Physics
Interplanetary Physics Branch
Greenbelt, Maryland 20771

SUBMITTED TO: Journal of Geophysical Research

Abstract

92% of the intense magnetic fields ($> 13\gamma$) observed at 1 AU during solar cycle 20 (1973-1975) were associated with shocks, stream interfaces, or cold magnetic enhancements (CMEs). Most (52%) of the magnetic field intensity enhancements occurred at stream interfaces; 27% occurred behind shocks without interfaces; and 11% occurred in CMEs. The most intense fields (25γ to 37γ) followed shocks, and they probably resulted from the combined effects of shock compression, stream compression and intense fields carried from the sun by the piston. Magnetic field intensities at interfaces did not exceed 25γ , suggesting a mechanism such as a magneto-acoustic wave limits the intensity ahead of streams. The intensities in CMEs did not exceed 20γ . Intense magnetic fields persisted longest behind shocks, presumably because pistons carry intense magnetic fields from the sun.

During a quiet period (1973-1975) interface-associated enhancements occurred 3.5 times as frequently as shock associated enhancements, and during an active period (1967-1969) shock-associated enhancements occurred 1.2 times as frequently as interface-associated enhancements. The frequency of CMEs did not change with solar activity. The absolute occurrence frequency of interface-associated enhancements increased by a factor of 2.4 in going from the active period to the quiet period, while the absolute occurrence frequency of shock-associated enhancements decreased by a factor of 1.7 in going from the active to the quiet period.

INTRODUCTION

Intense interplanetary magnetic fields are of basic importance to solar wind physics, magnetospheric physics and cosmic ray physics. They can exert an appreciable pressure on interplanetary flows; they are particularly effective in producing geomagnetic activity; they play an important role in the modulation of galactic cosmic rays; and they are probably an important factor in the propagation of solar energetic particles. It has long been known that intense magnetic fields can be produced by shocks and by streams. Recently, it has been shown that they can also occur in slow, cold flows which are sometimes found ahead of high speed streams. A systematic search for still other types of magnetic field enhancements has not been made.

A number of basic questions concerning the characteristics of intense interplanetary magnetic fields remain unanswered, despite numerous publications discussing individual events. Are there types of magnetic field intensity enhancements other than the three mentioned above? What are the greatest intensities that can be produced by shocks, streams, etc. within 1 AU? What is the distribution of maximum magnetic field intensities for each type of enhancement at 1 AU? What is the relative frequency of shock-associated magnetic field intensity enhancements, stream-associated enhancements, etc.? Does this relative frequency change with solar cycle? What are the plasma characteristics associated with intense magnetic fields? This paper aims to answer these questions using hourly averages of the magnetic field observed at 1 AU. The results

will also serve as a reference point for statistical studies of radial variations of intense magnetic fields measured by deep space probes such as HELIOS and VOYAGER.

2. DEFINITION AND CLASSIFICATION OF INTENSE MAGNETIC FIELDS

Our definition of intense interplanetary magnetic fields at 1 AU is based on a composite set of hourly averaged field intensities obtained from 9 IMP/AIMP spacecraft and from 2 HEOS spacecraft between late 1963 and early 1977. Distributions of the available 71,431 hourly values of B and of $\log B$ are shown in Figure 1. The distribution of B is asymmetrical and has a mean value of 6.09. The distribution of $\log B$ is similar to a normal distribution; the mean is 0.746 ($\log^{-1} 0.746 = 5.57$), and the rms deviation is 0.182. The finite width of these distributions results from the spatial and temporal variations of boundary conditions at the coronal source of the solar wind flow and from the action of interplanetary dynamical processes.

This paper addresses only the high end of the magnetic field intensity distribution. We define intense fields as those for which $\log B$ exceeds its mean value by at least 2σ , i.e., $B \geq 13\gamma$. There are 2096 such hours in the composite data set. Usually, intense fields persist for several hours and can be recognized as distinct events, which we refer to as magnetic field intensity enhancements or simply "magnetic enhancements".

Magnetic field intensity enhancements can be classified on the basis of their relations to plasma parameters (density, n ; temperatures, T ; and bulk speed, V). We shall show that magnetic enhancements belong to one of four categories:

1. Enhancement associated with stream interfaces (Belcher and Davis, 1971; Burlaga, 1974; Gosling et al., 1978).
2. Those which are associated with fast forward shocks but not with interfaces (Hirshberg and Colburn, 1969; Schatten

and Schatten, 1972; Chao and Lepping, 1974; Burlaga 1975; Hundhausen 1972; Dryer 1975

3. Those which can be identified as cold magnetic enhancements (Burlaga et al., 1974), and
4. Enhancements which are not associated with a shock, interface, or CME.

The presence of shocks, interfaces, or CMEs was determined from plots of hourly averages of the plasma and magnetic field data compiled by King (1977) for the period November 1963 through December 1975. We considered only those events for which nearly complete sets of field and plasma data are available.

Shock associated intensity enhancements are easy to recognize because a fast forward shock is characterized by a simultaneous increase in V , n , T , and B . Two examples of such enhancements are shown in Figure 2. (The configurations behind the shocks will be discussed below). Interface-associated intensity enhancements are also easy to recognize, because interfaces are characterized by an abrupt decrease in n , and a simultaneous increase in T and V . An example is shown in Figure 3. Usually, the magnetic field intensity is maximum at the interface. Interface-associated enhancements may be divided into two classes-those preceded by non-linear pressure waves or shocks (Figure 4), and those without such waves (Figure 3). Since we used hourly averages, we could not distinguish between shocks and non-linear pressure waves.

CMEs are readily identified because they occur where the temperature is extremely low, usually in low speed regions ahead of streams. An example is shown in Figure 5. The largest peak in B in Figure 5 may be

due in part to a compression resulting from the velocity gradient in the stream, but the intense fields in the low temperature region where the speed is constant or decreasing may be classified as a CME. Note the unusual field directions in the CME, suggesting a loop or bottle configuration.

We compiled a list of all (149) magnetic field intensity enhancements with adequate data coverage, in the period 1964-1975, and we classified them according to the categories listed above. Table 1 shows the results of our classification. 90% of the magnetic enhancements fell uniquely into one of the first three categories, i.e. they were associated with a shock or an interface or a CME. 8% of the enhancements could not be associated with a shock, a CME, or a stream interface. 2% of the events involved a combination of a CME, a shock, and/or an interface.

Table 1 shows that more than half (52%) of the magnetic enhancements occurred at an interface. One fourth of these were accompanied by a shock or non-linear pressure wave. Presumably these interface-associated enhancements were caused by the steepening of streams from coronal holes. 27% of the magnetic enhancements occurred near fast forward shocks that were not accompanied by an interface. These were probably caused by plasma emitted by solar flares or other transient events. 11% of the magnetic enhancements occurred in CME's. The cause of these enhancements is not known.

3. PHYSICAL CHARACTERISTICS OF REGIONS WITH INTENSE MAGNETIC FIELDS

This section discusses the distribution of maximum magnetic field intensities; the distribution of the durations of magnetic enhancements; and the distribution of V , n , and T for each of the principal types of magnetic field intensity enhancements (near shocks, near interfaces, and in CMEs). These results are essential for understanding the processes which cause intense interplanetary magnetic fields.

The distribution of maximum magnetic field intensities for the three principal types of magnetic field enhancements is shown in Figure 6. The highest magnetic field intensities observed at 1 AU were associated with shock waves. In fact, with one exception, all fields $> 25\gamma$ (i.e., greater than the mean plus 3.5σ) were associated with shock waves. The largest hour average magnetic field intensity ever recorded at 1 AU is 44.8γ ; this feature was also observed in association with a shock on August 4, 1972, by the Pioneer spacecraft (Dryer et al., 1976). Since we have no data at 1 AU for this event, it is not considered in our analysis. The most intense magnetic field that was observed in any of the enhancements that we studied is 37γ , which corresponds to the average magnetic field intensity logarithm plus 4.5σ . The data for that event (January 13, 1967) are shown in Figure 2. Note that:

- a) the speed in the flow behind the shock is relatively low ($< 500\text{km/s}$),
- b) the density and temperature in the magnetic enhancement are relatively high, and
- c) the densities in the flow behind the magnetic enhancement are exceptionally low.

Qualitatively similar profiles were observed in other post-shocks flows,

but there are differences in details. This is illustrated by the second event in Figure 2, where the intense magnetic fields were in a narrow piston of exceptionally hot and dense plasma. The intense magnetic fields associated with fast forward shocks at 1 AU probably result from three effects:

1. the magnetic fields in the piston itself are probably carried out from an intense field region on the sun and are therefore more intense than average;
2. these fields are further intensified by compression at the shock; and
3. ambient fields in front of the piston are compressed by the advance and steepening of the piston.

The intensity of magnetic fields associated with interfaces did not exceed 25γ (Figure 6). All available models suggest that those enhancements are produced by the kinematic steepening of a stream and that their intensity is limited by the propagation of a magnetoacoustic pressure wave away from the interaction region. (Rosenbauer et al., 1977; Gosling et al., 1978; Pizzo and Burlaga, 1977). These effects are apparent in the example shown in Figure 4. The intense fields are confined to the regions where the speed is increasing; the front and rear of their enhancement are steep, and they are correlated with large gradients in n , V , T , which correspond to pressure waves. The results in Figure 6 provide a strong constraint on such models: they must be capable of producing intensities as high as 13 to 25γ , but the maximum intensities should not exceed 25γ at 1 AU. Interfaces with shocks or non-linear pressure waves had a slightly greater field intensity than interfaces without such waves.

In CMEs the largest intensity (19 γ) was relatively low compared to that for the other types of enhancements discussed above (Figure 6), but the most probable intensity was relatively high (16 γ). CMEs are possibly the result of special source on the sun or a dynamical interaction near the sun, but the actual cause is unknown.

Let us now consider the distribution of the durations of magnetic enhancements. It was suggested above that intense fields in pistons behind shocks might be drawn out from intense field regions on the sun, whereas those associated with interfaces are produced by compressing the ambient interplanetary plasma. If this were the case, one would expect that the duration of intense magnetic fields would be longer in shock-associated enhancements than in interface-associated enhancements, because in shock-associated enhancements the duration is related to the width of the entire stream piston, whereas in interface-associated enhancements the duration is related to the width of the "front" of the stream (the region where V is increasing). Figure 7 shows the distribution of durations of events with $B \geq 13\gamma$ for enhancements near shocks and for enhancements near interfaces. There is some subjectivity in this figure due to small data gaps, but it probably does not affect the distributions very much. The expected difference is evident. The duration of the magnetic enhancements at interfaces is usually < 4 hr, and it is < 16 hrs in any case. By contrast the duration behind shocks has a much flatter distribution, showing that durations between 4 hrs and 17 hrs are nearly as common as durations < 4 hrs; furthermore intense magnetic fields lasting as long as 16 - 24 hrs are sometimes observed behind shocks.

Finally, let us consider the distributions of plasma parameters (V , n , T) corresponding to the maximum intensity in each of the magnetic field intensity enhancements that we identified. These are shown in Figure 8. For comparison, we note that the averages and rms deviations of V , $\log n$, and $\log T$, for all of the data in the composite data set are 448 ± 114 km/sec, 0.76 ± 0.30 , and 4.90 ± 0.33 , respectively. The corresponding n and T values are 5.75 cm^{-3} and $0.79 \times 10^5 \text{ }^\circ\text{K}$. (Average n and T values are 7.33 cm^{-3} and $1.04 \times 10^5 \text{ }^\circ\text{K}$, but the n and T distributions are more closely log-normal than normal, as has already been demonstrated for B.)

CMEs are very distinct in that the temperatures are usually $< 5 \times 10^4 \text{ }^\circ\text{K}$ and the speeds are relatively low (Of course, these are the characteristics used to identify them). The densities are higher than average in most CMEs, suggesting that they are related to non-compressive density enhancements (NCDEs) (Gosling et al., 1977). Another feature suggesting a link between CMEs and NCDEs is that both are typically found to be precursors of high speed streams. However note that some CMEs have $n < 9 \text{ cm}^{-3}$, and Gosling et al., have noted that NCDEs do not always have intense magnetic fields. The density and temperature distributions are similar in magnetic field enhancements at shocks and at interfaces with and without shocks. In most cases, the densities and temperatures are significantly higher than the average n and T in the solar wind. This is probably the result of the compressions produced by the kinematic steepening of streams and by the shocks. The average and most probable speed in magnetic field intensity enhancements at shocks are higher than

in enhancements at interfaces. This is because interfaces occur just ahead of streams where the speed is low (they mark the forward boundary of a stream) whereas in the case of shocks, the field intensity and speed maxima often occur simultaneously.

The event counts of Table 1 and of Figures 6-8 show minor variability because for a few events, data were adequate for one purpose (e. g. event classification) but not for another (e. g. event duration determination).

4. SOLAR CYCLE VARIATIONS

Ideally, one would like to determine the absolute rate of occurrence of each type of magnetic enhancement as a function of time for a typical solar cycle. This cannot be done with the available data for two reasons. First, the solar cycle for which the data are available was not typical in that geomagnetic activity, and by implication solar wind bulk speeds, were unusually high in the late phase of the cycle (Gosling et al., 1977). Secondly, data gaps prevent a determination of absolute occurrence rates.

For each year between 1963 and 1973, Barouch and King (1975) determined the relative occurrence frequency of magnetic enhancements lasting at least three hours. They did not have an extensive plasma data base available and could not categorize enhancements by type, as is done in this paper. With a 15% threshold for event selection, they showed local maxima in the years 1966, 1970, and 1972.

It is our intent to focus on two phases of the past solar cycle, one (1967-1969) generally associated with high sunspot number and much transient solar activity, and the other (1973-1975) associated with low sunspot number, less transient solar activity, and the occurrence of long lived high speed streams. For brevity we refer to these periods as "active" and "quiet", respectively, although each period had both flares and streams.

We are interested in determining the extent to which the mix of enhancement types differs for these two periods and the extent to which the distribution of maximum field intensities varies.

The results are summarized in Table 2. For the quiet period, the most common type of enhancements were those associated with interfaces

(57%); they occurred 3.5 times as frequently as shock-associated enhancements. For the active period, the most common type of enhancement was the shock-associated enhancement, which occurred 1.2 times as frequently as interface-associated enhancements. The higher relative frequency of shocks during the active period supports the view that shocks which are not associated with interfaces are due to ejecta from active regions. It is significant that during the active period the interface associated enhancements occurred nearly as often as the shock associated enhancements.

Table 2 shows that there was no change between the active and quiet periods in the following:

1. the sum of the percentages of enhancements at shocks and at interfaces;
2. the percentage of CMEs; and
3. the percentage of events with no interface, shock or CME.

Note from Table 2 that the occurrence frequency of all types of magnetic enhancements was 1.4 times greater during the quiet period than during the earlier period. The occurrence frequency of interface-associated enhancements increased by a factor of 2.4 in going from the active to the quiet period, while the occurrence frequency of shock associated enhancements decreased by a factor of 1.7. These results are normalized in that the percent of all hours with field and plasma data is similar for the two periods (60% vs 63%), and the data gap distributions are not very dissimilar. However, these numerical results may not be typical of active period vs quiet period comparisons. This may be seen from the result of Barouch and King (1975) that the annual occurrence rates for all ($> 15 \gamma$)

enhancements fluctuates by a factor of 2 over the 1966-1972 period, with minimal values obtained in 1967-1969 and in 1971.

The predominance of shock-associated enhancements during active periods may explain why the modal magnetic field intensity is somewhat higher at solar maximum than at solar minimum (Neugebauer, 1975; Hirshberg, 1973), since shock-associated enhancements have exceptionally large magnetic field intensities. This implies that the magnetic field intensity distribution should have a larger "tail" at solar maximum, as is observed (Hirshberg, 1969).

Does the maximum magnetic field intensity at interfaces or at shocks change appreciably with solar cycle? We have calculated the average B_{\max} for both types of enhancements with $B_{\max} > 13\gamma$. For shock-associated enhancements, $\langle B_{\max} \rangle = 19.9\gamma$ in 1967-1969 and $\langle B_{\max} \rangle = 19.8\gamma$ in 1973-1975. In the interface-associated enhancements, $\langle B_{\max} \rangle$ was 15.9γ for the active period and 16.9γ for the quiet period; this difference is not very large, considering that the 1973-1975 streams were generally much faster and longer lasting than the streams of the earlier period.

5. SUMMARY AND CONCLUSIONS

Interplanetary magnetic field and plasma data for a period exceeding one full solar cycle were examined for intervals in which the magnetic intensity exceeded 13γ . This threshold corresponds to $\langle \log B \rangle + 2\sigma$. 149 such intervals were found with nearly complete plasma and magnetic field data. Most (79%) of these enhancements could be associated either with interplanetary shocks or with high speeds stream interfaces. Half of the remaining 21% of the enhancements could be identified as cold magnetic enhancements (CMEs) while the other half could not be associated with a single shock, interface, or CME. When the threshold for selection of a magnetic enhancement is increased to $\langle \log B \rangle + 3\sigma$ ($\approx 19\gamma$), all enhancements are shock or interface associated.

Distributions of maximum magnetic field intensities and of the durations for the principal types of enhancements are consistent with shock-enhancements being due in part to the drawing out of intense fields from the solar atmospheric shock-initiation neighborhood, while the interface-enhancements involve just compressions of interplanetary fields in front of the streams. The distribution of interface associated intensities suggests the action of some mechanism (e. g. magnetoacoustic pressure waves) which limits these intensities to $\leq 25\gamma$. In fact, in about 25% of the interface associated enhancements, a feature consistent with a nonlinear magnetoacoustic pressure pulse is observed.

We compared the relative occurrence rates of magnetic enhancements observed during the periods 1967-1969 and 1973-1975. Interface-associated enhancements were strongly dominant in the latter period, while shock-

associated enhancements were weakly dominant in the former. These results are consistent with the latter period being dominated by high speed streams emanating from long-lived coronal holes and the former period having contributions both from the transient flows from active regions and from flows from quasi-stationary sources. Enhancements of all types were more frequent, by a factor of ≈ 1.4 , for the 1973-1975 period than for 1967-1969. The maximum field values associated with both shocks and stream interfaces showed no significant difference in the two periods considered. Cautions in interpreting the numerical results of this comparison as typical solar cycle variations were stressed.

We note that the galactic cosmic ray intensity at 1 AU was higher in 1973-1975 than in 1967-1969, even though there were more magnetic field enhancements in the former period. In other words, cosmic rays were modulated more when there were fewer enhancements. Yet Barouch and Burlaga (1975) found that individual magnetic enhancements generally are associated with depressions in cosmic ray intensity. Evidently the nature of magnetic enhancements is more important than the total number of enhancements in modulating cosmic rays. The modulation was greatest in the active period when most enhancements were associated with shocks, and it was least when in the quiet period when most enhancements were associated with interfaces. This is consistent with Liouville's theorem which implies that transient disturbances (such as shock-associated enhancements) should be more effective modulating agents than nearly stationary disturbances (such as interface-associated enhancements). Thus the 11 year cosmic ray cycle is probably primarily the result of the cumulative effect of the 11-year variation of the number of transient interplanetary magnetic field configurations.

TABLE 1

CLASSIFICATION OF MAGNETIC FIELD INTENSITY ENHANCEMENTS

<u>Magnetic Enhancements</u>	<u>1965 - 1975</u>
Near interface	52%
(without pulse)	(39%)
(with pulse)	(13%)
Near shock (no interface)	27%
Cold magnetic enhancement	11%
No interface, shock CME	8%
Multiple interface, shock, CME	2%
Number of events	149

TABLE 2

SOLAR CYCLE VARIATION OF MAGNETIC ENHANCEMENTS

<u>Intense Magnetic Field</u>	<u>Active Sun (1967-1969)</u>	<u>Quiet Sun (1973-1975)</u>
Near interface	34%	59%
(without pulse)	(30%)	(43%)
(with pulse)	(4%)	(16%)
Near shock (no interface)	41%	17%
Cold magnetic enhancement	11%	10%
No interface, shock, CME	9%	10%
Multiple interface, shock, CME	4%	3%
Number of events	48	67

FIGURE CAPTIONS

- Figure 1. Distributions of 71,431 hourly averaged values of B , and of their logarithms, as measured between late 1963 and early 1977. Note the separate linear and logarithmic abscissae. Note that the rightmost B bin is an integral bin.
- Figure 2. Two examples of interplanetary shock associated magnetic enhancements. Hourly averages of magnetic field magnitude B and plasma parameters bulk speed (V), ion density (n), and ion temperature (T) are shown. The solid vertical lines show the shock arrivals at the observing spacecraft. The dashed vertical line indicates the end of the shocked plasma regime.
- Figure 3. Example of a magnetic enhancement associated with a high speed stream interface. The interface is defined as the region, bounded by the vertical lines, between the density and temperature maxima. Note that the interface region precedes the speed maximum and that the magnetic field is not significantly enhanced after the interface passes. The stepped appearance of the plasma parameters for the January 28 - February 4 period results from the use of three hour averages.
- Figure 4. Another example of an interface-associated magnetic enhancement. This example differs from that of Figure 3 in that here a nonlinear pressure wave (left vertical dashed line) is observed to precede the interface (bounded by the solid and right dashed vertical lines). The feature visible on July 4 - 5 is a shock associated magnetic enhancement.

Figure 5. Example of a cold magnetic enhancement. Note the largest peak may be due in part to compression by the stream, but there are intense fields in the region of low temperature where the speed is constant or decreasing, which is characteristic of CMEs.

Figure 6. Histograms of magnetic field maxima for principal types of magnetic enhancements. Numbers of enhancements of each type are shown.

Figure 7. Histograms of magnetic enhancement durations for shock associated and interface associated enhancements. No durations >24 hours were observed.

Figure 8. Histograms for three plasma parameters (V , T , n) for each of the principal types of magnetic enhancements.

REFERENCES

- Barouch, G., and L. F. Burlaga, Causes of Forbush decreases and other cosmic ray variations, J. Geophys. Res., 80, 444, 1975.
- Barouch, E. and J. H. King, A survey of the interplanetary magnetic field, Proc. of the 14th International Cosmic Ray Conf., 3, 1036, 1975.
- Belcher, J. W., and L. Davis, Jr., Large-amplitude Alfvén waves in the interplanetary medium, 2, J. Geophys. Res. 76, 3534, 1971.
- Burlaga, L. Interplanetary stream interfaces, J. Geophys. Res., 79, 3717, 1974.
- Burlaga, L., Interplanetary streams and their interaction with the earth, Space Sci. Rev., 17, 327, 1975.
- Burlaga, L. N. F. Ness, F. Mariani, B. Bavassano, U., H. Rosenbauer, R. Schwenn, and J. Harvey, Magnetic fields and flows between 1 AU and 0.3 AU during the primary mission of Helios 1, J. Geophys. Res., in press 1978.
- Chao, J. K. and R. P. Lepping, A correlative study of ssc's, interplanetary shocks, and solar activity, J. Geophys. Res., 79, 1699, 1974.
- Dryer, M. Interplanetary shock waves--Recent developments, Space Sci. Rev., 17, 277, 1975.
- Dryer, M., Z. K. Smith R. S. Steinolfson, J. D. Mihalov, J. M. Wolfe, and J. K. Chao, Interplanetary disturbances caused by the August 1972 solar flares as observed by Pioneer 9, J. Geophys. Res., 81, 4651, 1976.

- Gosling, J. T., J. R. Asbridge, and S. J. Bame, An unusual aspect of solar wind speed variations during solar cycle 20, J. Geophys. Res., 82, 3311, 1977.
- Gosling, J. T., J. R. Asbridge, S. J. Bame, and W. C. Feldman, Solar wind stream interfaces, J. Geophys. Res., 83, 1401, 1978.
- Hirshberg, J., Interplanetary magnetic field during the rising part of the solar cycle, J. Geophys. Res., 74, 5814, 1969.
- Hirshberg, J. The solar wind cycle, the sunspot cycle, and the corona, Astrophys. Space Sci., 20, 473, 1973.
- Hirshberg, J., and D. S. Colburn, Interplanetary field and geometric variations a unified view, Planetary Space Sci., 17, 1183, 1969.
- Hundhausen, A. J., Coronal Expression and Solar Wind, p. 169, Springer Verlag, New York, 1972.
- King, J. H., Interplanetary Medium Data Book, NSSPC/WDC-A-R&S, 77-04, 1977.
- Neugebauer, M., Large-scale and solar cycle variations of the solar wind, Space Sci. Rev., 17, 221, 1975.
- Pizzo, V., and L. Burlaga, The dynamics of steep stream configurations near the sun, Eos, 58, 1225, 1977.
- Rosenbauer, H., R. Schwenn, E. Marsch, B. Meyer, H. Miggenrieder, M. D. Montgomery, K. H. Mulhauser, W. Pilipp, W. Voges, and S. M. Zink, A survey on initial results of the HELIOS plasma experiment. J. Geophys. 42, 561, 1977.
- Schatten, K. H. and J. E. Schatten, Magnetic field structure in flare-associated solar wind disturbances, J. Geophys. Res., 77, 4858, 1972.

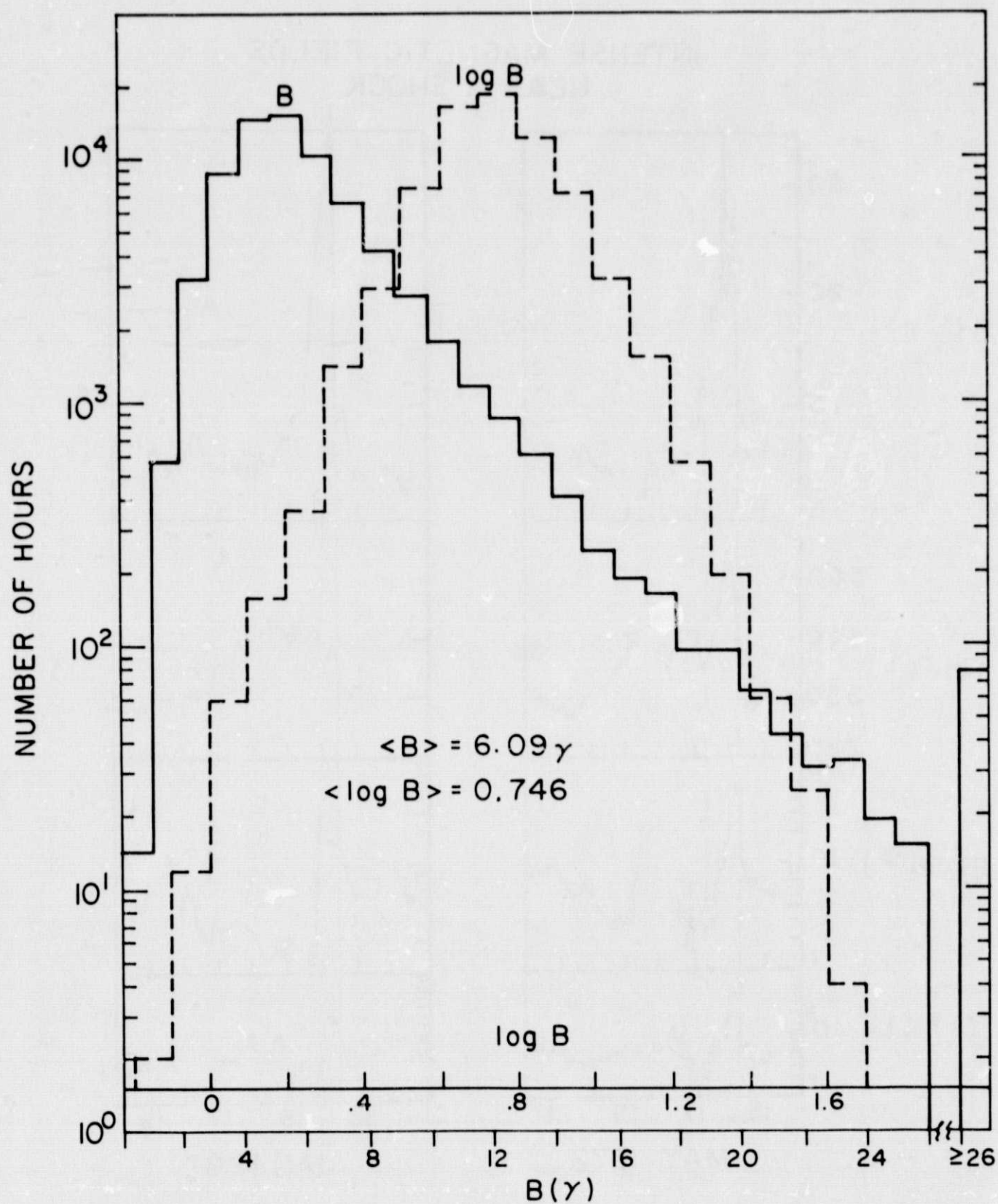


Figure 1

INTENSE MAGNETIC FIELDS NEAR A SHOCK

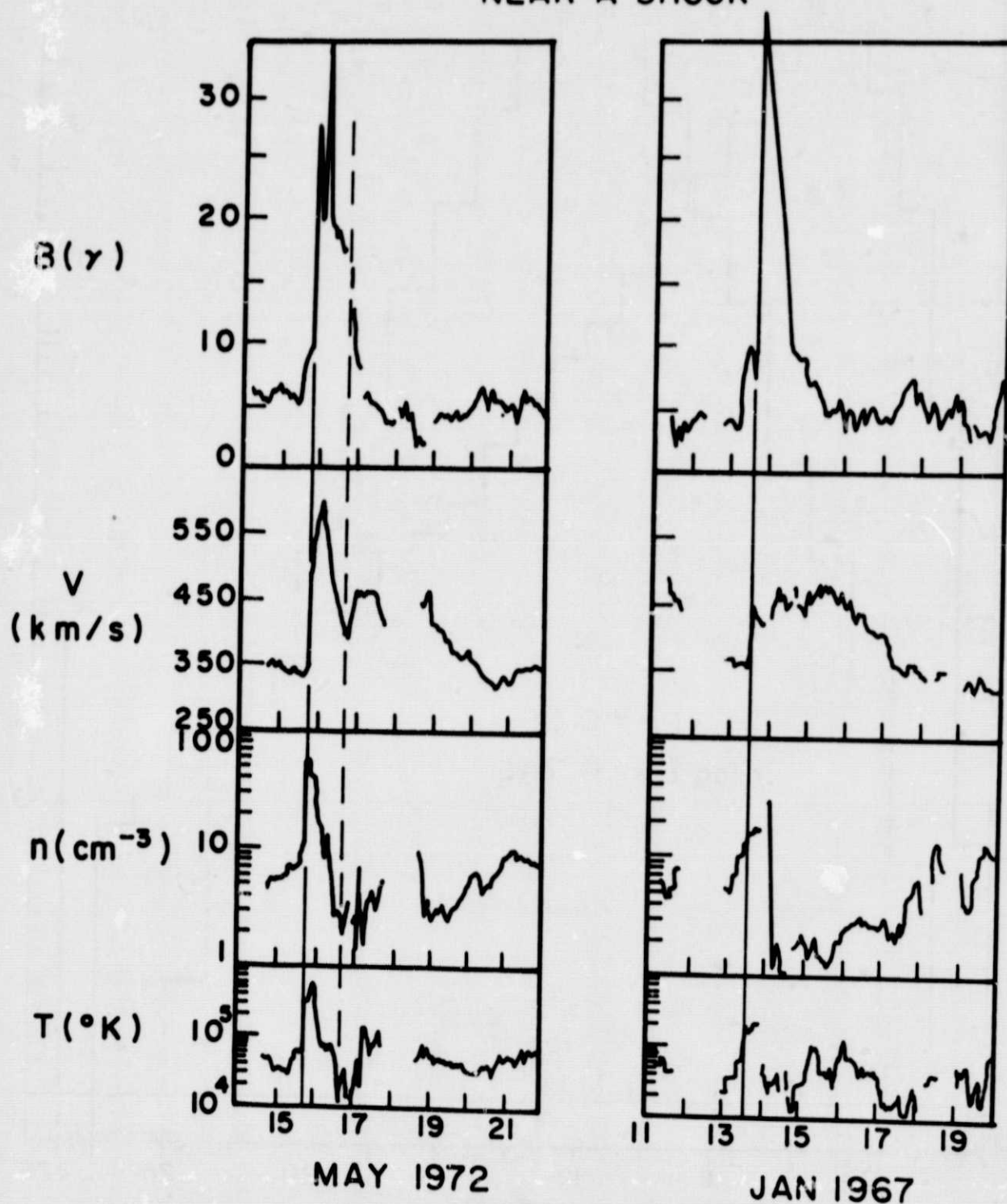


Figure 2

ORIGINAL PAGE IS
OF POOR QUALITY

INTENSE MAGNETIC FIELDS NEAR AN INTERFACE

NO SHOCK

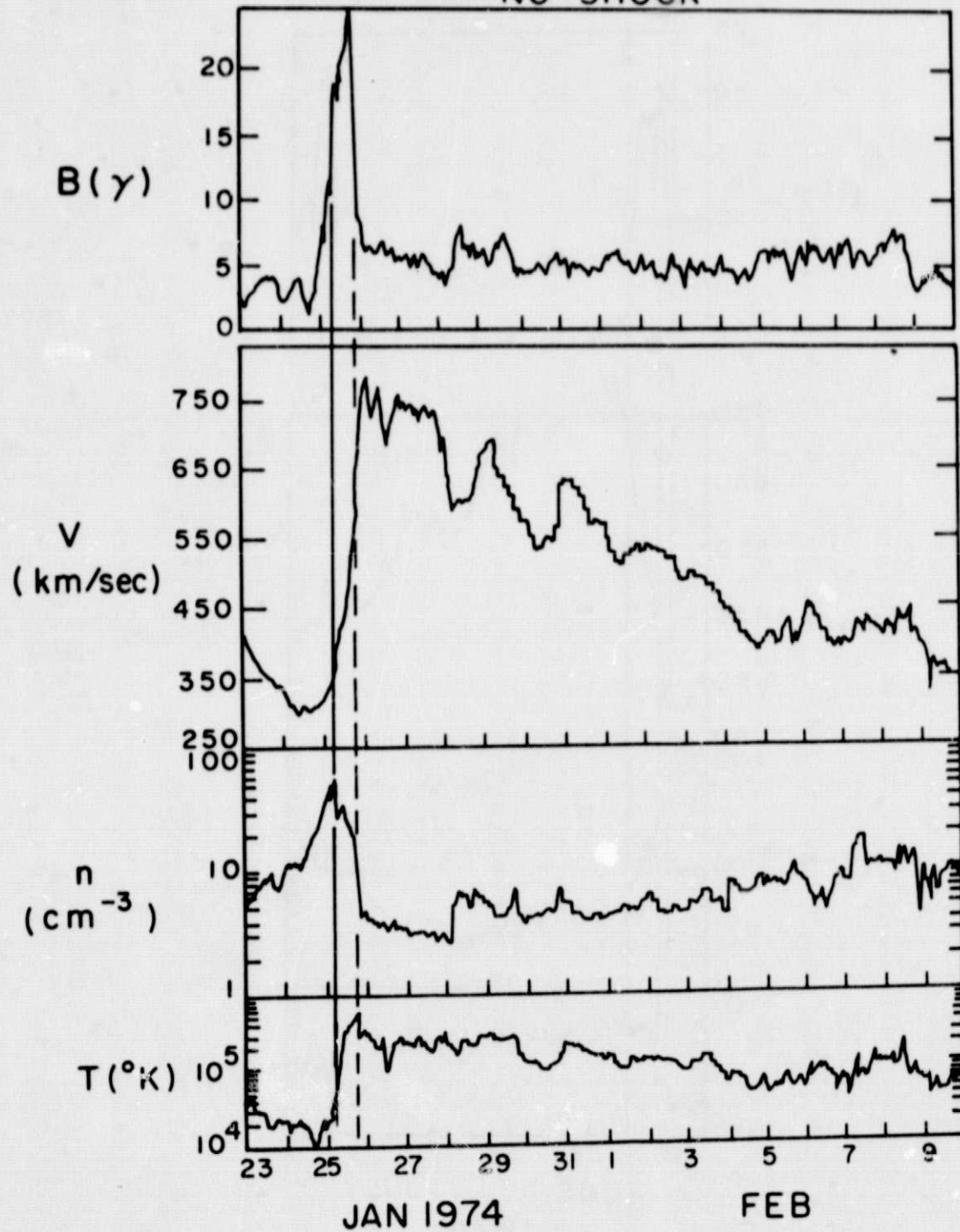


Figure 3

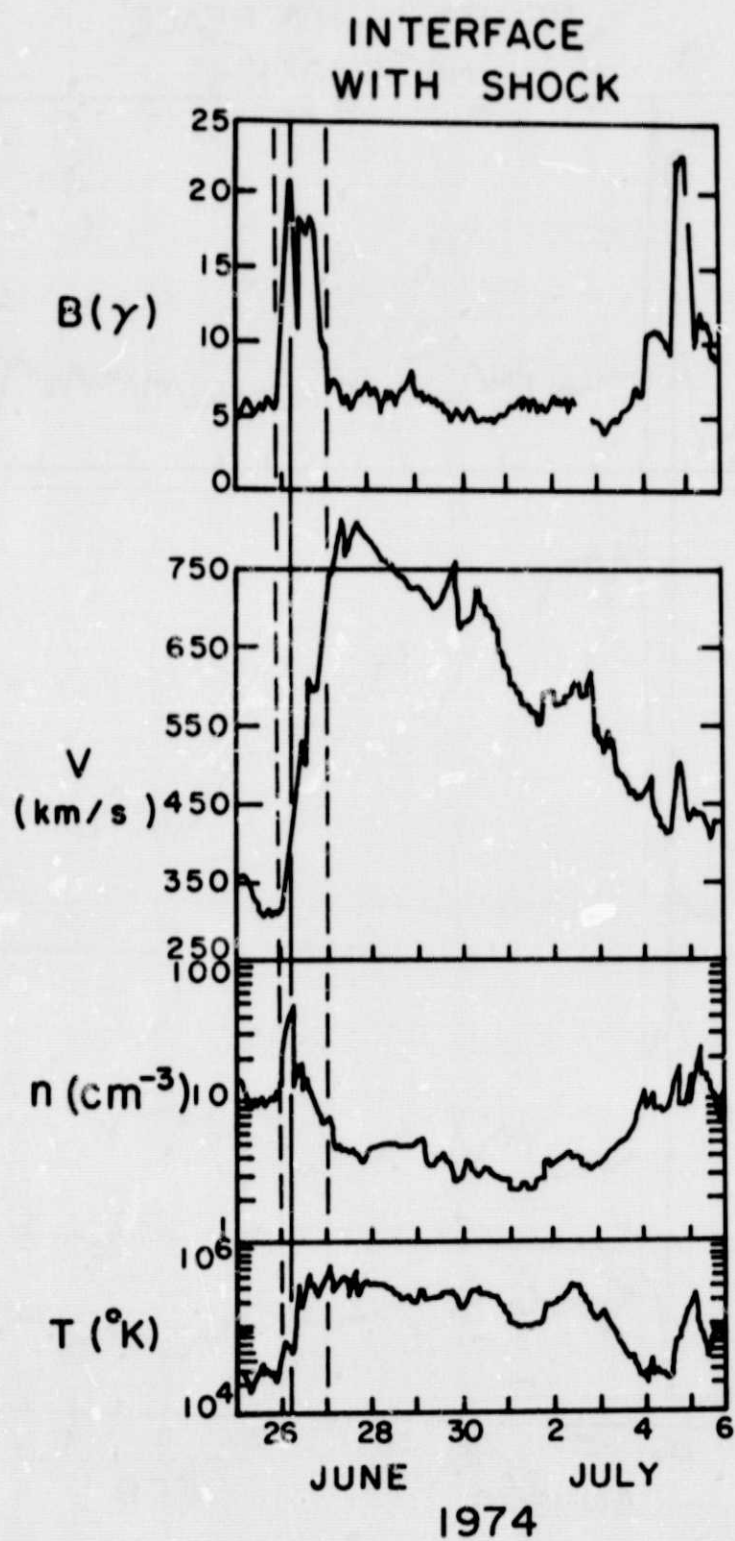


Figure 4

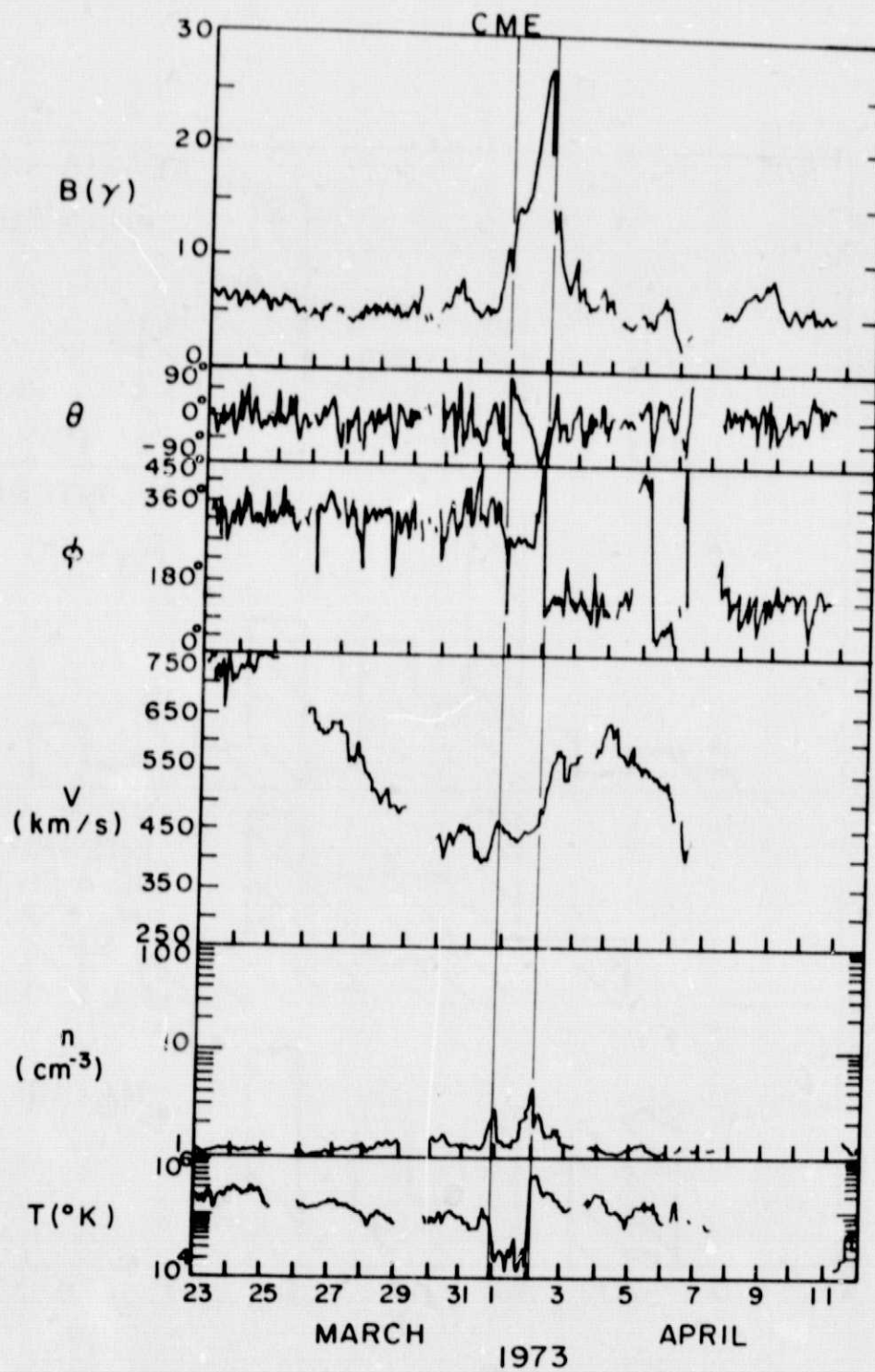


Figure 5

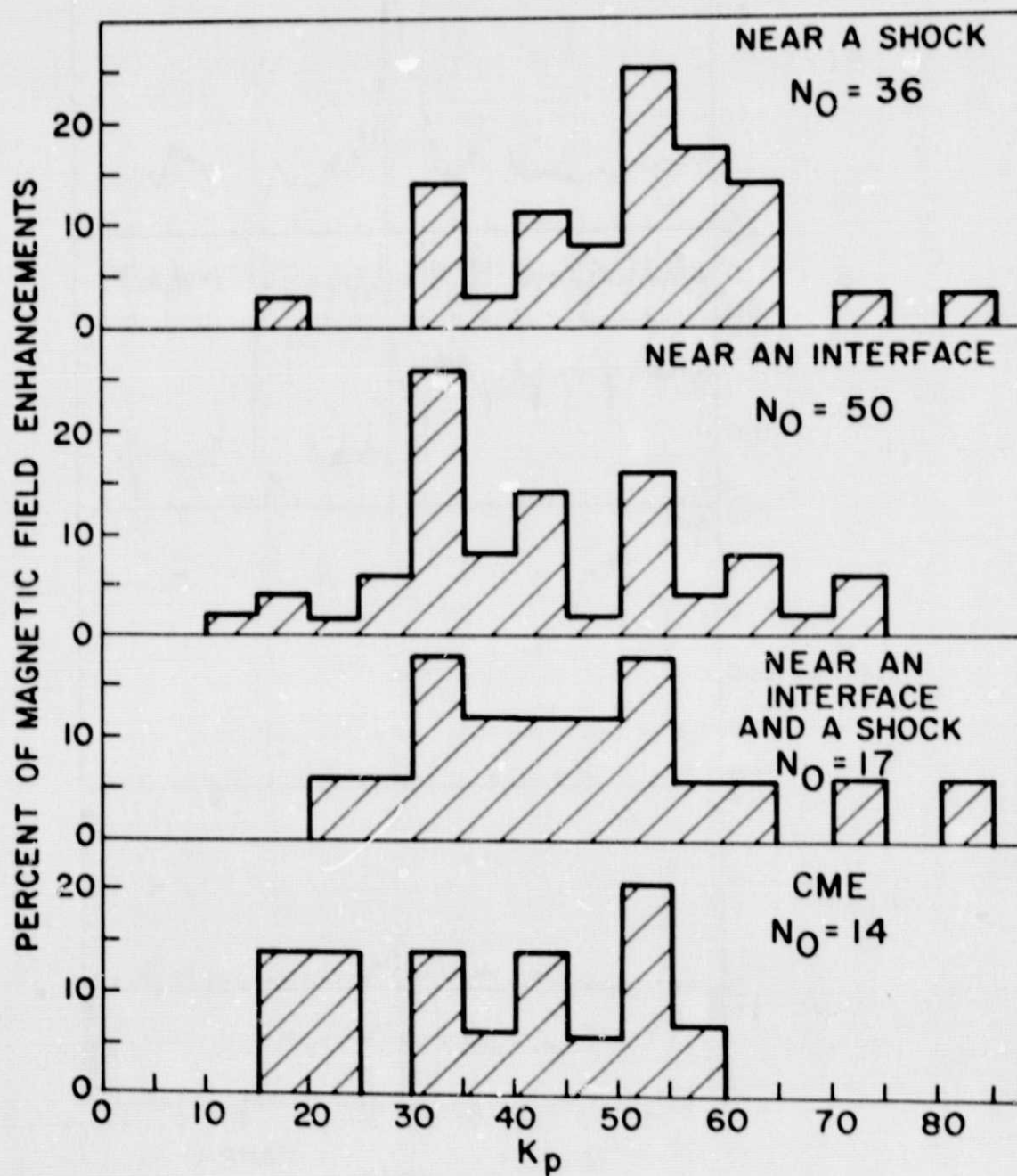


Figure 6

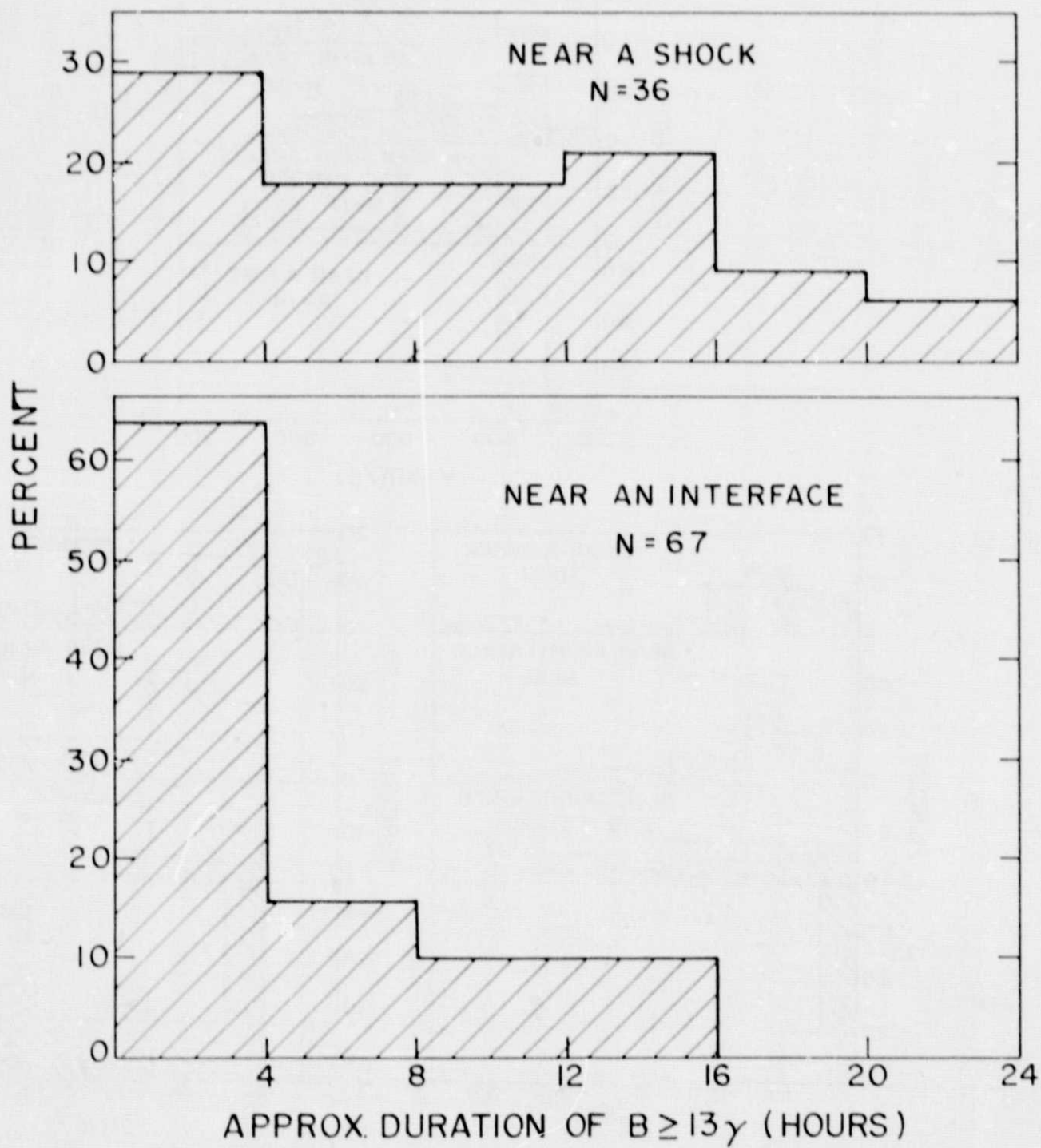


Figure 7

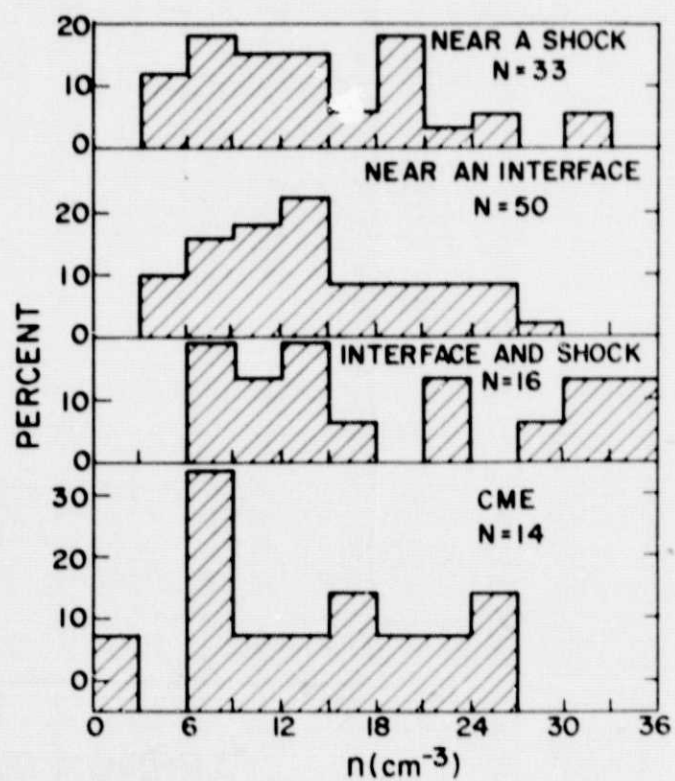
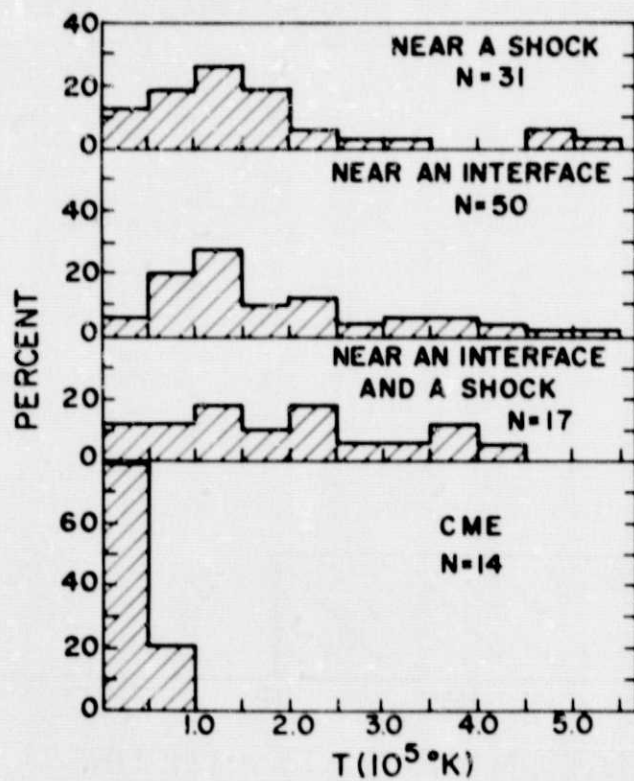
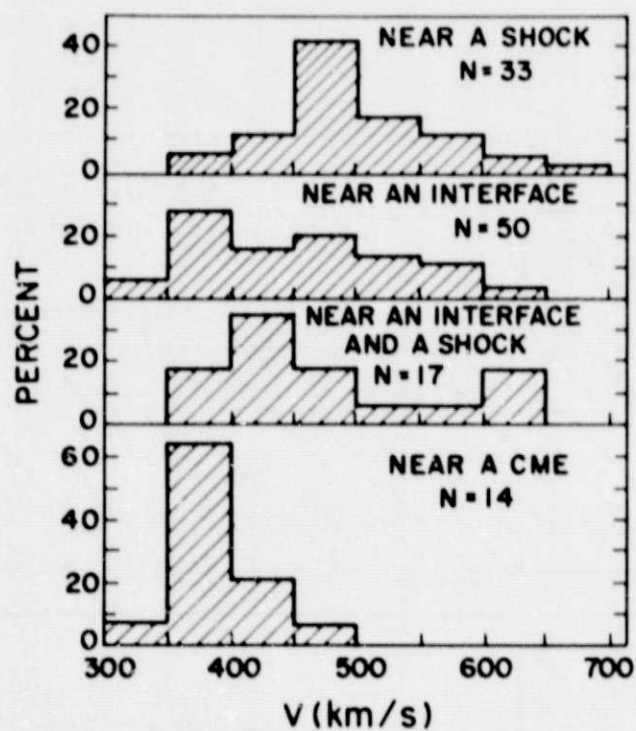


Figure 8